COMMUNICATIONS PHYSICS

ARTICLE

https://doi.org/10.1038/s42005-019-0204-y OPEN

Unraveling the thermodynamic conditions for negative gas adsorption in soft porous crystals

L. Vanduyfhuys [1] & V. Van Speybroeck [1]

Soft porous crystals (SPCs) are widely known for their intriguing properties and various counterintuitive phenomena such as negative linear compression, negative thermal expansion and negative gas adsorption (NGA). An intriguing case is the adsorption of methane in DUT-49 for which experimentally a drop in the amount of adsorbed particles was observed under increasing vapor pressure. It is yet unknown which specific systems can exhibit NGA under which thermodynamic conditions. Herein, a semi-analytical thermodynamic model is applied to determine the conditions required for NGA, including their sensitivity towards various system-specific parameters, and investigate the correlation with pressure-induced breathing. As such, it is found that certain non-breathing materials may exhibit breathing with NGA under application of a fixed mechanical pressure. Such meticulous control of multiple triggers for NGA can open the way to new applications such as tunable gas detection and pressure amplification.

[1] Center for Molecular Modeling (CMM), Ghent University, Technologiepark 46, 9052 Zwijnaarde, Belgium. Correspondence and requests for materials should be addressed to L.V. (email: Louis.Vanduyfhuys@UGent.be) or to V.S. (email: Veronique.Vanspeybroeck@UGent.be)

Metal–organic frameworks (MOFs) are among the most intriguing materials of current science, mainly due to their hybrid nature as they are made up from metal ions or metal clusters linked together by organic linkers[1–4]. These materials were already identified as interesting candidates in the context of various applications such as mechanical shock absorbers[5], controlled drug release[6] as well as storage and separation of gases[7–9]. Even though flexibility and crystallinity are usually perceived as counterintuitive, it was discovered that some MOFs show "flexible" behavior in the sense that they are capable of transforming between various phases accompanied by substantial changes in the unit cell volume (up to 40%) while retaining their structural integrity. Kitagawa coined the term "soft porous crystals" (SPC) for materials that show a bistable or multistable behavior with long–range structural order and permanent porosity[10]. The phase transitions can be triggered by various external stimuli such as mechanical pressure, temperature, electric fields, light or gas adsorption[11,12]. Being built partly out of weaker interactions (dispersive interactions, $\pi - \pi$ stacking, hydrogen bonds), their response upon such stimuli can be uncommon compared to traditional microporous materials[11,13–15]. Anomalous mechanical properties have been discovered such as negative linear compressibility (NLC), where upon hydrostatic compression, the system expands along one or more directions instead of contracting[16,17]. Under influence of temperature, negative thermal expansion (NTE) was discovered, where materials contract upon heating rather than expanding[18,19]. Although NTE was discovered before in zeolites and other molecular frameworks[20], it occurs in a large temperature range and with a large amplitude in MOFs[21]. Under influence of gas adsorption, negative gas adsorption (NGA) was recently discovered where at some point the MOF releases gas from its pores when the vapor pressure of the surrounding adsorbate is increased[22]. Finally, in contrast to many cases of breathing where the adsorption isotherm contains a single transition step, N_2 adsorption in Co(bdp) displays a multistep adsorption isotherm figuring intermediate structures differing mainly in the linker orientation[23].

Recently, NGA was experimentally realized by Krause et al. for DUT–49 where adsorption of methane at a temperature of 120 K induces a sudden structural transition from an open–pore structure to a contracted–pore structure, together with a large drop in the amount of adsorbed methane (see Fig. 2 in ref. [22]). Furthermore, Evans et al. investigated the structural transition in more detail using molecular dynamics simulations and found that a molecular buckling of the organic linker results in a colossal framework transformation that allows for negative gas adsorption[24]. Furthermore, it has been demonstrated that bistability with large energetic barriers combined with large pore sizes are closely connected with NGA[25]. However, we still lack a fundamental understanding of the specific thermodynamic conditions that are required to observe NGA, which is prerequisite for the design and tuning of new state-of-the-art applications. Given the unique nature of NGA in which the material counteracts an external force applied to it, the ability to trigger NGA in a controlled fashion could give rise to an entirely new branch of applications such as gas-releasing rescue systems and a wide array of pneumatic devices[22,26–28]. From the experiments done so far, it is already clear that NGA can occur in certain materials, but it is still unclear whether from a fundamental theoretic point of view, the number of systems in which NGA could be observed can be expanded provided the thermodynamic conditions are right. Krause et al. found that DUT–48, a new material they synthesized which is very similar to DUT–49 but with a smaller linker, does not exhibit any breathing transitions and as a result, also no NGA[27]. They found that a stiffening of the framework (due to the smaller linker) with respect to DUT–49, in combination with a lower adsorption enthalpy of methane was responsible for the lack of transitions. The same group also observed that the structural transitions for nitrogen in DUT–49 critically depend on the particle size of the single crystals[28]. It was found that the particle size alters the complex structural transformation mechanism and yields multiple structural transformations figuring unprecedented intermediate structures.

Herein we formally want to investigate how materials respond upon exposure to varying environmental pressure. Such environmental pressure might be modulated either by changing the vapor pressure of an adsorbing gas and/or an additional mechanical pressure. In the current experimental setups, it would be very difficult to actually perform experiments that allow to decouple mechanical and vapor pressure. In existing experiments where a mechanical pressure is applied to a MOF powder, a pressure transmitting medium is used (such as mercury or silicon oil), which occupies the space between MOF crystals and therefore makes it very difficult for an adsorbing gas to ever reach the MOF material. Scientists are also attempting to embed MOF material in so-called mixed-matrix membranes[29]. Although these materials may possibly allow to apply mechanical pressure by other means, such as diamond anvils, such experimental setups are still unavailable. The research proposed here applies a thermodynamic model to give fundamental insight into the thermodynamic triggers required for NGA, even if those triggers are experimentally not easily accessible. In this sense it might be seen as a thought experiment. To set the scene, we first consider a hypothetical system, albeit strongly inspired by methane adsorption in DUT–49. We propose a general picture of the conditions under which NGA might occur, including the sensitivity of these conditions towards various system-specific parameters. Afterwards, we compare the response of various types of SPCs to investigate the correlation between the pressure-induced breathing of the frameworks with the adsorption-induced breathing at fixed mechanical pressure. Finally, we use the insight gained from performing such thought experiments to better understand the experimental observations indicating that certain systems exhibit NGA in the absence of mechanical pressure, while others do not. We show that such insights may be used to modulate a material towards NGA conditions even in the absence of mechanical pressure.

Results

Context. In this work we want to obtain fundamental insight into the conditions that trigger negative gas adsorption. Negative gas adsorption is usually percieved as extraordinary and counterintuitive, which results from the application of the second law of thermodynamics to the grand canonical adsorption isotherm. Considering adsorption of guest molecules by an adsorbent at constant volume and temperature, the second law dictates that the amount of adsorbed guests should always increase with increasing vapor pressure. In other words the slope of the grand canonical adsorption isotherm should always be positive (derivation given in Supplementary Note 1):

$$\left(\frac{\partial N}{\partial p}\right)_{V,T} = \frac{1}{\rho(p,T)\cdot\left(\frac{\partial^2 F}{\partial N^2}\right)_{V,T}} > 0 \qquad (1)$$

where p and ρ represent respectively the vapor pressure and the density of the gas reservoir and F represents the Helmholtz free energy of the adsorbent–adsorbate system. However, this expression is only valid under conditions of fixed unit cell volume, in other words, for rigid adsorbents. Whenever the adsorption of guest molecules induces changes in the volume of the adsorbate, the expression given above is formally no longer valid. However, for flexible adsorbents featuring a continuously

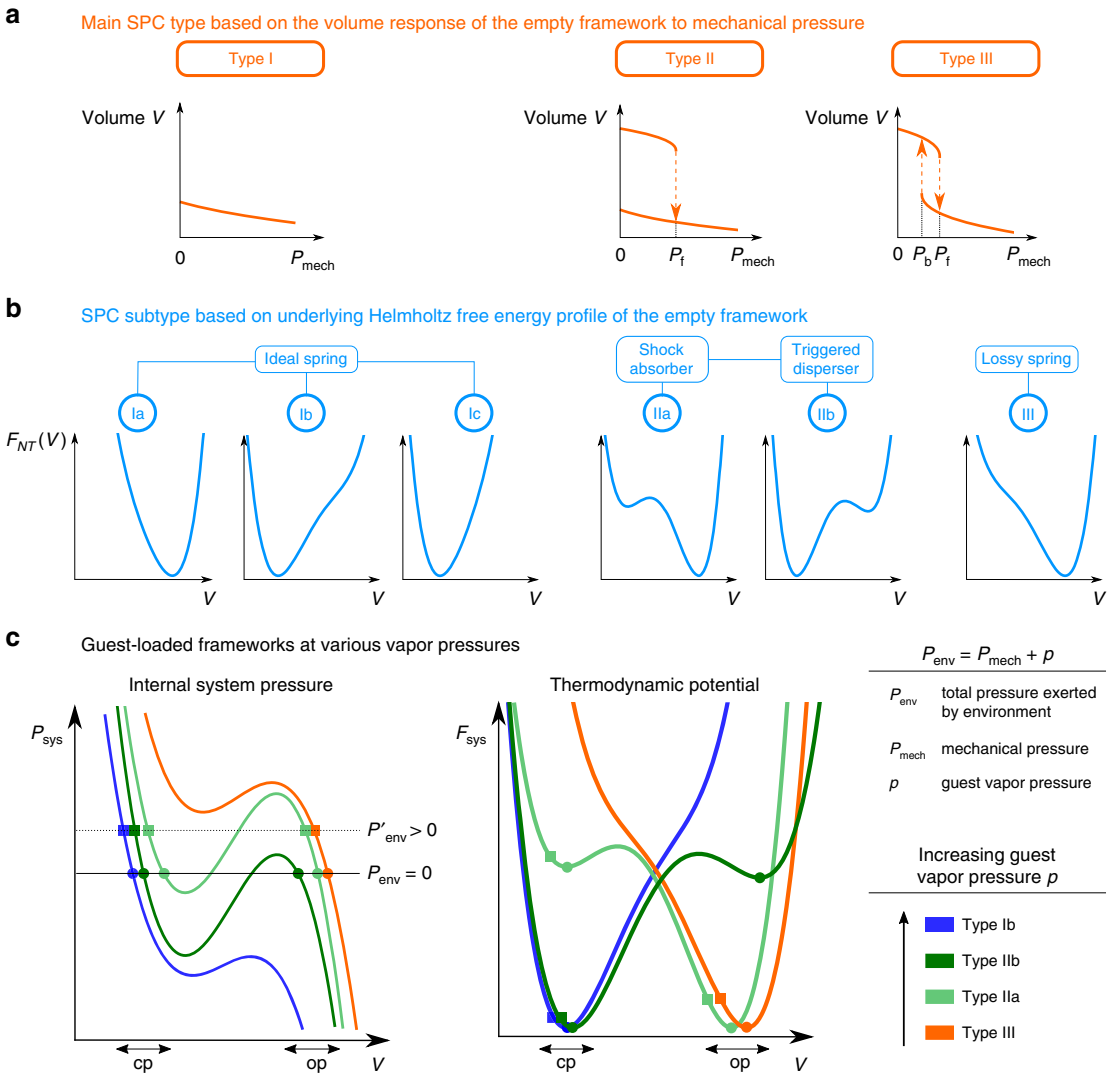

Fig. 1 Illustration of soft porous crystal (SPC) types and their correlation with the thermodynamic potential of guest-loaded frameworks. **a** Definition of main SPC types based on the pressure-induced breathing behavior **b** Distinction between subtypes based on the empty-host free energy profile respectively (**c**) The internal system pressure and corresponding thermodynamic potential for guest-loaded frameworks. The intersection with the horizontal lines illustrate the mechanical equilibrium in case the environment exerts no mechanical pressure ($P_{env} = 0$), as well as when it exerts a positive pressure ($P_{env} > 0$). Finally, open pore (op) and closed pore (cp) phases are indicated. This figure was adapted from ref. [30] (L. Vanduyfhuys et al., "Thermodynamic insight into stimuli-responsive behavior of soft porous crystals", Nat. Commun., 2018) licensed under a Creative Commons Attribution 4.0 International License

varying volume, i.e., without discontinuous phase transitions, a similar expression can be derived (see Eq. 31 of Supplementary Note 1), indicating NGA will occur if $\frac{\partial^2 F}{\partial V^2} + \rho(p,T) \cdot \frac{\partial^2 F}{\partial N \partial V} < 0$. Even though this relation does not universally forbid NGA for such flexible adsorbents, it still points towards positive gas adsorption in the known SPCs. In contrast, for an adsorbent undergoing a discontinuous phase transition between metastable states, one cannot rely on these expressions anymore to make a statement whether or not NGA is forbidden, indicating the crucial role of such phase transitions for the observation of NGA. Finally, Krause et al. even showed that NGA cannot take place at global thermodynamic equilibrium, but necessarily involves a metastable phase (see supporting information of ref. [22]).

In a recent contribution of the present authors, a generalized thermodynamic approach was proposed to classify SPCs into various types upon exposure of mechanical pressure[30]. The cornerstone for the classification is the Helmholtz free energy profile of the empty framework. Three main types could be identified as schematically illustrated in Fig. 1a. Type I materials feature no transition triggered by mechanical pressure. Type II exhibit irreversible transitions, i.e., the material does not return to the initial state after releasing the pressure. Type III show a reversible transitions, i.e., the material does return to the initial state. Based on the underlying Helmholtz free energy profile, as indicated in Fig. 1b, type II materials are further divided in type IIa, for which the large pore is more stable and will absorb mechanical energy upon contraction (shock absorbers), and type IIb, for which the narrow pore is more stable and will release energy (triggered disperser). Here, we wish to build further upon this partitioning and investigate whether there is a correlation between pressure-induced breathing of the empty framework, i.e., the type of the material, and adsorption-induced breathing at fixed mechanical pressure. In this light, Fig. 1c illustrates how the internal system pressure as well as the corresponding thermodynamic potential could change for a varying vapor pressure p of an adsorbing guest species. Adsorption-induced breathing

transitions can be identified by considering the mechanical equilibrium with the total pressure exerted by the environment $P_{env} = P_{mech} + p$, which can be modulated by changing either the mechanical pressure P_{mech} or the vapor pressure p. Such equilibrium is found when the system pressure equals the environmental pressure. This is indicated in Fig. 1c as the intersect of the system pressure profile with a horizontal line at the corresponding value of P_{env} with the extra condition that the system pressure has a negative slope to ensure mechanical stability. As can be derived from the figure, at some vapor pressures the system has stable equilibria at both open pore (op) and contracted pore (cp) phases (eg. the green curves), while at other vapor pressures only one stable phase is found (blue and orange curves). If one starts for example under conditions where two minima are possible (eg. dark green curve), but by varying the environmental pressure (from $P_{env} = 0$ to $P'_{env} > 0$ as indicated on the figure) one minimum disappears, a possible phase transformation might occur.

Thermodynamic model. From a thermodynamic point of view, the fundamental quantity dictating the response of the system upon external stimuli, is the thermodynamic potential. Considering the system under conditions of fixed number of host unit cells n, adsorbate molecules N, unit cell volume V and temperature T, such potential is given by the Helmholtz free energy F. This Helmholtz free energy is the starting point of the current investigation and consists out of 3 ingredients as schematically illustrated in Fig. 2: the empty host free energy, the guest–guest interactions inside the pores and the guest–host interaction[31]. However, to translate the model towards realistic experimental conditions of fixed adsorbate chemical potential μ (or equivalently fixed vapor pressure p) as well as fixed environmental pressure P_{env}, we need to perform a Legendre transform of the Helmholtz free energy (in the N, V, T ensemble) to the osmotic potential X (in the μ, P_{env}, T ensemble). This transformation is summarized in the Methods section, while further details can be found in Supplementary Note 2 and ref. [31]. By performing this Legendre transformation, one can also identify possible phase transitions. In this work, collective behavior is assumed in which each unit cell has to act simultaneously during a phase transition[31]. Such collective behavior implies that the system is not necessarily in the global thermodynamic equilibrium, but will instead be in a metastable state whenever it is seperated from the global equilibrium by a non-zero barier in free energy. This has two important implications. On the one hand, metastable states are crucial for the observation of NGA as was pointed out by Krause et al.[22]. On the other hand, an op-to-cp phase transition will occur under influence of guest adsorption only if the metastable op-phase disappears at a certain value of the vapor pressure, forcing the system to transition to the global equilibrium given by the cp-phase.

The guest–guest interactions in the model are described using the van der Waals equation of state, which is in principle only reliable for temperatures above the critical temperature. Multiple studies are available in literature which examine phase transitions in nanopores at subcritical temperatures in terms of capillary condensation[32–34]. In this context, classical density functional theory (cDFT) is appropriate to account for the inhomogeneous density profile[35]. It was found that, depending on the pore size, the adsorption uptake exhibits hysteresis in terms of the applied chemical potential[36]. For the MOFs considered here, this implies that the isotherm could not only exhibit hysteresis in terms of transitions between states with various volumes, but also in terms of states with various uptakes at fixed volume. To fully understand the capillary phase transitions in MOFs at subcritical conditions and its associated hysteresis patterns, one would require to perform a dedicated study of its own (more details can be found in the Supplementary Note 5). Evans et al. applied cDFT in which MOFs are treated as simple slit pores with a string attached to its walls to investigate possible negative gas adsorption and found a correlation between NGA on the one hand, and bistability, large pore volumes and subcritical temperatures on the other hand[25]. However, in this work, we limit ourselves to consider supercritical conditions, and show that it still allows for NGA given that the thermodynamic conditions are right.

Thermodynamic conditions for NGA in DUT-49 type materials. NGA for methane in DUT–49 was observed experimentally at 120 K, which is below the critical temperature of methane of 192 K. Therefore, we start our investigation for a hypothetical system in which we modified the van der Waals a parameter of methane so that its critical temperature becomes 80 K. As a result, one has to remain careful in treating this system as a true model for CH_4 in DUT-49. Afterwards, the impact of modifying the a parameter and other system parameters will be evaluated (*vide infra*). In this work, we specifically investigate how the breathing and adsorption behavior is affected by the application of a mechanical pressure P_{mech} on top of the vapor pressure p exerted by the adsorbate. An additional P_{mech} implies that the system is in mechanical equilibrium with an environment exerting a pressure of $P_{env} = P_{mech} + p$. Figure 3 shows the adsorption isotherm for the hypothetical system introduced earlier, i.e., the amount of adsorbed species as function of the vapor pressure p, at various mechanical pressures P_{mech}. These plots contain both the number of species adsorbed in the open pore phase (op, indicated in blue in Fig. 3a–d) as well as in the contracted pore phase (cp, indictated in red in Fig. 3a–d). If at a given vapor pressure a certain phase is missing, it is due to the fact that that particular phase is no longer (meta)stable at the given vapor pressure. As a result, one can deduce whether or not breathing will occur as well as if it is

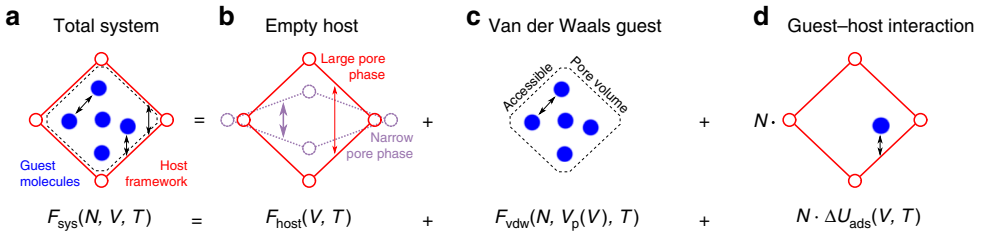

Fig. 2 Illustration of the mean-field thermodynamic model used in this work. The total system Helmholtz free energy F_{sys} (**a**) in terms of number of adsorbed guest molecules N, the unit cell volume V and temperature T, is expanded within a mean-field model into (**b**) an empty host free energy F_{host}, (**c**) van der Waals contribution F_{vdw} for the guests confined within the pores with volume V_p and (**d**) an interaction term ΔU_{ads} describing the adsorption energy of a single molecule with the framework

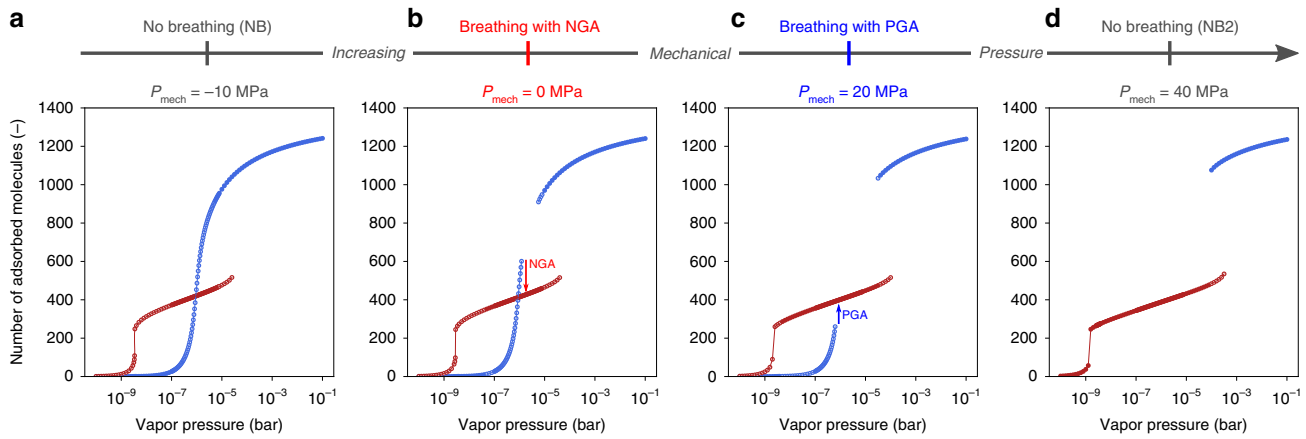

Fig. 3 Adsorption isotherm for the hypothetical system (inspired by CH_4 gas in DUT-49) at 120 K and fixed mechanical pressure. The blue and red dots represent the number of molecules adsorbed in the open pore and contracted pore state respectively. The mechanical pressure is set to **a** −10 MPa with no breathing observed (NB), **b** 0 MPa exhibiting breathing with negative gas adsorption (NGA) corresponding to the experimental observations, **c** 20 MPa exhibiting breathing with positive gas adsorption (PGA) and **d** 40 MPa with no op-to-cp breathing transition (NB2)

accompagnied with negative or positive gas adsorption. An op-to-cp transition, i.e., from the open pore to the contracted pore, occurs if the op state suddenly ceases to exist because it becomes thermodynamically unstable. Furthermore, NGA can be identified as a drop in the amount of adsorbed guests across the breathing transition. We first consider panel (b) as it represents the adsorption isotherm in absence of mechanical pressure and can therefore be directly compared with the experiments performed by Krause et al.[22]. As can be derived from the figure, the material undergoes a phase transition from the contracted pore to the open pore in which the amount of adsorbed methane decreases, in other words negative gas adsorption occurs. Therefore, the predictions of the model presented here are in aggreement with experimental observation of NGA in DUT-49 without mechanical pressure[22]. If we now consider the subsequent application of increasing mechanical pressure from −10 MPa to 40 MPa, we can conclude that, depending on the mechanical pressure, the material can exhibit one of four different responses. Panel (a) represents adsorption with negative mechanical pressure $P_{\mathrm{mech}} = -10$), and no breathing transitions are observed. In panel (b), no mechanical pressure is applied ($P_{\mathrm{mech}} = 0$), and corresponds to a breathing transition with NGA in agreement with experiment as mentioned before. Panel (c) represents adsorption at an applied mechanical pressure of $P_{\mathrm{mech}} = 20$ MPa, again resulting in a breathing transition from op to cp, but this time with positive gas adsorption. Finally, panel (d) represents adsorption for an even higher mechanical pressure of $P_{\mathrm{mech}} = 40$ MPa, which reveals there is no longer an op-to-cp transition triggered by gas adsorption. This is due to the fact that the mechanical pressure is higher than the transition threshold for the empty host (wich is 38 MPa according to the force field applied in this work). Hence, at this mechanical pressure and at a vapor pressure of $p = 0$ bar, the system is already in a contracted pore state, and no op-to-cp breathing transitions will be observed for increasing vapor pressures. For the remainder of this work, it is usefull to interpret the behavior under applied mechanical pressure by considering that in terms of the op-to-cp transition, applying positive mechanical pressure can be viewed as making the framework more flexible, while applying a negative mechanical pressure can be viewed as making it more rigid. In this regard, the material doesn't breath at −10 MPa since the negative mechanical pressure stiffens the material too much.

Impact of external mechanical pressure on breathing and NGA. The pressure sweep performed in the previous section describes the response of the system from a fundamental theoretical point of view and indicates that the considered system exhibits negative gas adsorption in the absence of mechanical pressure, but switches to positive gas adsorption at elevated mechanical pressure or no breathing at negative mechanical pressures. It is now important to investigate what the extent is of these NGA and PGA windows in terms of the applied mechanical pressure. To this end, we consider the internal system pressure P_{sys} in the grand canonical ensemble as function of the vapor pressure p and the unit cell volume V as obtained through a Legendre transform (see the Methods section), which is plotted in Fig. 4a. If we now first consider the equilibrium in the absence of mechanical pressure (i.e., the horizontal line at $P_{\mathrm{mech}} = 0$ MPa as indicated on Fig. 4a), we observe that for the empty host (gray dashed line) as well as for low vapor pressures (yellow line), there is an intersection at the open pore volume and hence a stable open pore phase. However, at increased vapor pressure (orange line), this intersection dissappears, implying that the open pore phase vanishes and the system is forced to transition to the contracted pore phase. In other words, an op-to-cp phase transition occurs in absence of mechanical pressure. Moreover, if we investigate the pressure profiles $P_{\mathrm{sys}}(p, V)$ more closely for various vapor pressures, we observe that the local maximum close to the op phase first decreases with increasing vapor pressure until it reaches its lowest value of −5 MPa (orange line), after which it increases again. This implies that, if we apply a negative mechanical pressure, i.e., consider the intersect with a horizontal at a negative external pressure, an adsorption-induced transition will only be observed while the mechanical pressure remains higher than −5 MPa. This is indeed confirmed by the adsorption isotherm shown previously in Fig. 3a corresponding to a mechanical pressure of −10 MPa, which does not exhibit breathing anymore. Finally, if we increase the mechanical pressure above 38 MPa, which is the local maximum for the empty host (i.e., the dashed curve), the empty host will already undergo a pressure-induced transition to the empty cp. This implies that there is no adsorption-induced transition, which is also confirmed by the adsorption isotherm shown previously in Fig. 3d.

At this point, we can conclude that the system will exhibit an adsorption-induced breathing transition from op to cp, if a mechanical pressure is applied between −5 MPa and 38 MPa. To deduce whether NGA or PGA occurs, we need to determine the

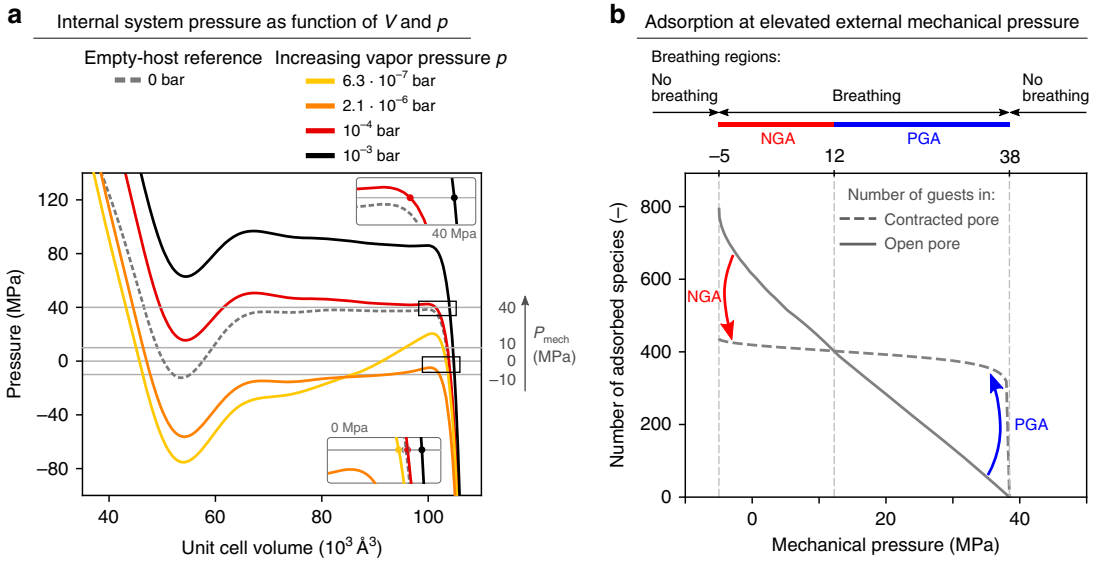

Fig. 4 Profiles related to adsorption in the hypothetical system inspired by CH_4 in DUT-49 at 120 K. **a** Grand canonical pressure as function of unit cell volume V for several fixed values of the vapor pressure p. The intersect with the horizontal lines (and with a negative slope) indicate equilibrium with the corresponding mechanical pressure P_{mech}. The inset figures show the mechanical equilibria at mechanical pressures of 0 and 40 MPa. **b** Number of guests adsorbed in the open pore prior to (dots), as well as in the contracted pore posterior to (dashes) a possible op-to-cp breathing transition as function of the mechanical pressure P_{mech}. Various regions are identified and shown at the top: no breathing (NB), negative gas adsorption (NGA) and positive gas adsorption (PGA)

number of guests adsorbed in the op phase prior to the transition (N_{op}), as well as in the cp phase posterior to the transition (N_{cp}). These numbers are computed using the semi-analytical thermodynamic model through the application of Eq. 11 from the Methods section (see also Supplementary Note 2). The results are vizualised in Fig. 4b in which NGA or PGA can be identified when N_{op} is respectively larger or smaller than N_{cp}. To interpret the results, it is helpful to note that the vapor pressure p_t at which the op-to-cp transition occurs, decreases for increasing mechanical pressure P_{env}. Indeed, from Fig. 4a, we can derive that for a mechanical pressure of $P_{env} = -5$ MPa the transition occurs at $p_t = 2.1 \times 10^{-6}$ bar (orange curve), while for $P_{env} = 38$ MPa it occurs at $p_t = 0$ bar (dashed curve). For mechanical pressures beyond these limits, there is no transition. From Fig. 4b, we can now clearly identify 4 regions of varying adsorption behavior in terms of the mechanical pressure. (i) No Breathing (NB, $P_{mech} < -5$ MPa), for wich no adsorption-induced breathing transitions are observed, instead the framework remains in the op phase. The applied negative mechanical pressure is so large that it stiffens the framework to the point that it hinders guest adsorption to trigger the breathing transition. (ii) Negative Gas Adsorption (NGA, -5 MPa $\leq P_{mech} < 12$ MPa), for which an op-to-cp transition with negative gas adsorption is observed. The mechanical pressure has reached the threshold to stop hindering adsorption-induced breathing. Furthermore, the transition occurs at a large vapor pressure (due to a low mechanical pressure), which in turn results in a large number of guests adsorbed in the op, more then in the cp. (iii) Positive Gas Adsorption (PGA, 12 MPa $< P_{mech} <$ 38 MPa), for which an op-to-cp transition with positive gas adsorption is observed. The mechanical pressure has reached the threshold to stop hindering adsorption-induced breathing. However, the transition now occurs at a small vapor pressure (due to a high mechanical pressure), which results in a small number of guests adsorbed in the op, less then in the cp. (iv) No Breathing (NB2, 38 MPa $\leq P_{mech}$), for which no adsorption-induced op-to-cp transition is observed because even at low vapor pressure, the adsorbent is already in cp under influence of a mechanical pressure above the op-to-cp transition pressure of the empty framework.

Tuning breathing and NGA by varying system parameters. So far, we investigated a hypothetical system that is related to methane in DUT–49, even though it cannot be directly compared with the experimental measurements. Nevertheless, by investigating the sensitivity of the various regions observed for this system, we aim to gain insight into the generic features that influence the NGA phenomenon. To further investigate the sensitivity of these regions towards all system–specific parameters, such as host rigidity, adsorption interaction energy, pore volume and adsorbate van der Waals parameters, we modify each parameter and reconstruct the adsorption profile similar as in Fig. 4b. The results for the host rigidity and adsorption energy are shown in Fig. 5, whereas the other plots are shown in Supplementary Note 6. From Fig. 5a, we can see that increasing the host flexibility shifts all regions towards lower mechanical pressures. This can indeed be understood by recalling the physical meaning of the intersection of the N_{op} branch with the P_{mech}-axis, i.e., the pressure limit for which the empty op transitions towards the empty cp. Increasing the flexibility will decrease this limit and hence shift the curve towards lower mechanical pressures.

From Fig. 5b, we can deduce that increasing the adsorption interaction extends the NGA and PGA regions to lower pressures, while keeping the NB2 region intact. This can be rationalized as follows. Due to a higher adsorption energy of the guest molecules in the cp compared to the op, the guests prefer to adsorb in the cp phase. If we now increase the magnitude of the adsorption energy, this preference will increase even further. Therefore, the number of guests adsorbed in the op will decrease at fixed mechanical pressure while the number of guests in the cp increases. Indeed, this is confirmed by Fig. 5. Increasing the adsorption strength (going from lighter blue to darker blue) at fixed mechanical pressure decreases N_{op} (dots) and increases, albeit only very slightly, N_{cp} (dashes). The reason why N_{cp}

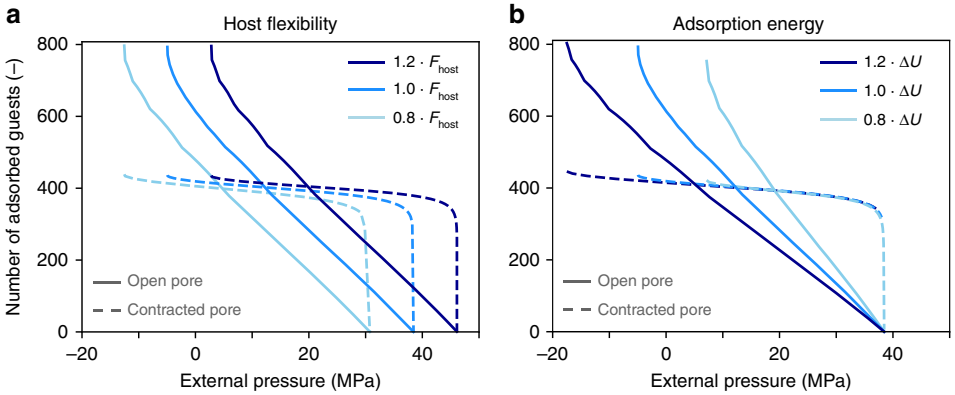

Fig. 5 Sensitivity of the various breathing regions when varying various contributions. **a** Sensitivity towards varying the host rigidity by scaling the empty host free energy F_{host}. **b** Sensitivity towards varying the adsorption energy ΔU. The solid line indicates the number adsorbed in the open pore phase prior to transition while the dashed line indicates the number adsorbed in the contracted pore phase posterior to transitions

increases only very slightly is because the cp is already almost fully filled at the point of transition. As a result, not much more molecules can adsorb extra due to the increased preference. Furthermore, the observed trend (i.e., the curve N_{op} becomes less steep with increased adsorption strength) is proven analytically in Supplementary Note 2.

These results also imply that the accuracy of the force field will have a non-negligible impact on NGA. For example, when the framework becomes 20% more rigid (curve for $1.2{\cdot}F_{host}$ in a), or the adsorption energy is decreased with 20% (curve for $0.8{\cdot}\Delta U$ in b), the system will no longer exhibit NGA in the absence of mechanical pressure. Finally, Supplementary Fig. 6 indicate that other system parameters, such as pore volume and guest van der Waals parameters, enable to modulate the NGA window further. For example, increasing the pore volume (as well as decreasing the van der Waals *b* parameter) tends to extend the NGA region towards lower pressures. Furthermore, it also increases the NGA magnitude, i.e., increases the drop in the amount of adsorbed particles. Finally, increasing the van der Waals *a* parameter again extends the NGA region towards lower pressures. Previous analysis clearly shows the sensitivity of the breathing and NGA window under various system parameters. Specifically, the host flexibility and adsorption energy turn out to have a large impact.

Exploring the NGA window in various SPC types. Given previous exploration on the behavior of a DUT-49 type material, belonging to the type IIa class, it is now interesting to apply the same procedure to other types of SPCs with a fundamentally different shape for the empty framework free energy profile, namely type IIb and III materials. As such, we investigate the correlation between the mechanical pressure-induced breathing behavior of the empty framework on the one hand (i.e., the type of the material as introduced in ref. [30]), and the adsorption-induced breathing behavior at fixed mechanical pressure on the other hand (i.e., the various breathing regions as introduced in the previous section). We consider three model systems: the system based on CH_4 in DUT-49 from the previous section for type IIa, CO_2/CH_4 in MIL-53(Al) for type IIb and CO_2/CH_4 in MIL-53(Cr) for type III. In contrast to the previously introduced hypothetical system, the input required for the other two models was taken directly from molecular simulations can therefore be considered as true models. More details on this input required for the thermodynamic model can be found in the Methods section. Figure 6 illustrates the adsorption-induced breathing behavior as function of the applied fixed mechanical pressure for the three types of SPCs. However, we now limit the discussion to positive mechanical pressures, which are experimentally accessible.

As the response of type IIa materials was already discussed in detail in the previous section, we now focus on type IIb and III materials. Considering first the breathing behavior of the type III material MIL-53(Cr) under adsorption of methane or carbon dioxde, we find that the distinction of the various breathing regimes is very similar as in type IIa materials (i.e NB, NGA, PGA and finally NB2). However, the interaction strength of CO_2 is so strong, that it extends the PGA region below 0 MPa, and as such effectively shifts the NGA region completely to negative pressures, which is experimentally not accessible. Methane on the contrary, which adsorbes less strongly in MIL-53(Cr), can induce NGA at a well chosen mechanical pressure between 30 and 43 MPa. To the best of our knowledge, there are no adsorption experiments performed yet that could confirm this hypothesis. Unfortunately, such experiments would be very difficult as they not only require to perform adsorption experiments in which a mechanical pressure is applied on top of the vapor pressure, the applied mechanical pressure also needs to be controlled in a highly accurate way to be able to identify all different breathing regions. However, as was mentioned before, the NGA region is also dependent on system-specific features. In this respect, the NGA region might shift or increase in pressure range if the system is slightly modified. An example for such modification might be a functionalisation of the linkers.

Finally, focussing now on the response of the type IIb material, we notice the introduction of a new region in between PGA and NB2, which will further be referred to as NGA2 and has a rather large window for methane (25–35 MPa) and a rather small window for carbon dioxide (34–35 MPa). The origin of this extra region is related to two aspects. First, the guest molecules adsorb in the contracted pore phase (cp) which has a higher volume than the empty closed pore phase (clp) of the empty framework (as indicated in Fig. 6) and is furthermore not a (meta)stable phase of the empty framework, i.e., not a (local) minimum in the free energy profile indicated in blue. Second, as was mentioned before, the vapor pressure of the op-to-cp transition decreases with increasing mechanical pressure. As a result, in the case of methane, when the mechanical pressure reaches a value between 25 and 35 MPa, the vapor pressure of the transition will be so low that the cp phase has not yet stabilized. Instead, the material will transition to the empty clp, which is too narrow to host any guests. Hence, since the amount of adsorbed guests drops from non-zero (in op) to zero (in clp), this region also represents negative gas adsorption and is therefore labeled NGA2. In case of CO_2, the same effect is at play, however, due to the larger adsorption energy of carbon dioxide, the cp phase stabilizes much faster resulting in a smaller window for NGA2.

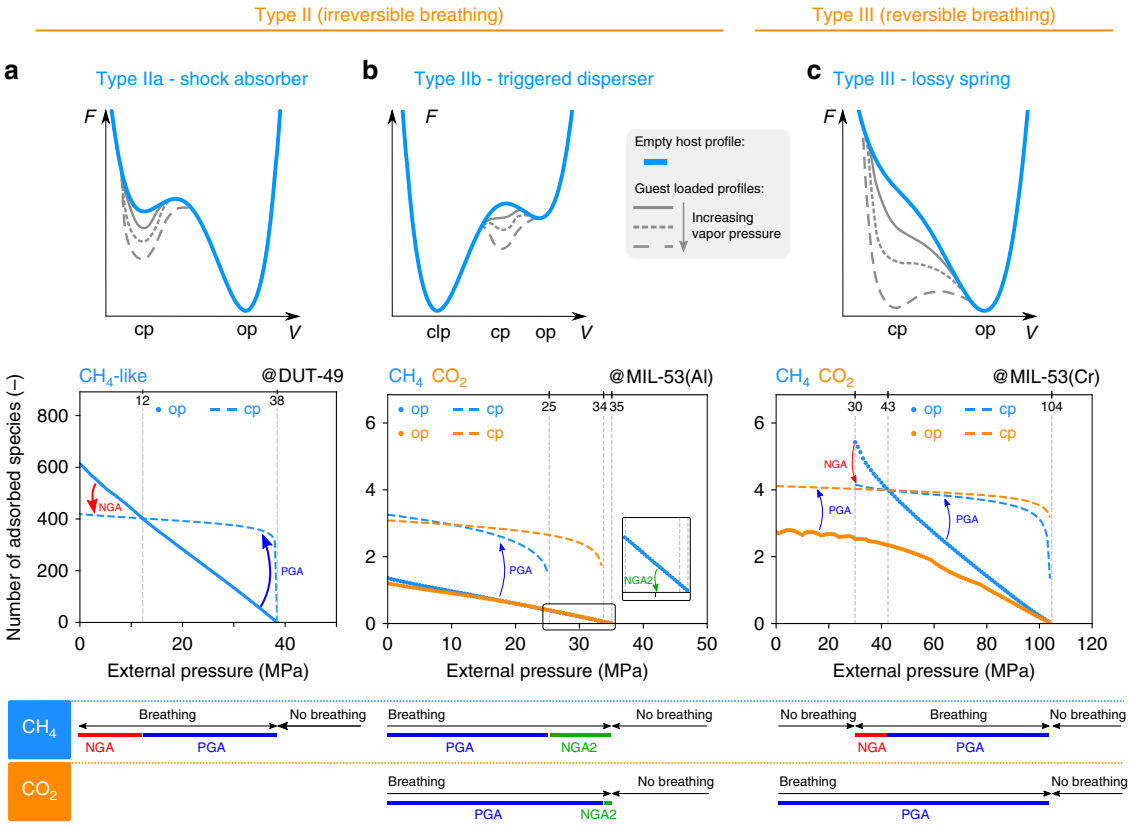

Fig. 6 Identification of the various regions of breathing for adsorption of methane (blue) and carbon dioxide (orange) in various types of SPCs. **a** A type IIa material (DUT-49), **b** a type IIb material (MIL-53(Al)) and **c** a type III material (MIL-53(Cr)). Dots and dashes represent the number of adsorbed guests in the open pore and contracted pore respectively during a possible op-to-cp breathing transition as function of the applied mechanical pressure P_{mech}

Discussion

By applying a thermodynamic model starting from the Helmholtz free energy of the host-adsorbate system, we observed that the adsorption-induced breathing behavior of soft porous crystals is subdivided in various windows in terms of the applied mechanical pressure. In case of type IIa and III materials, 4 of such windows are found. In increasing order of applied mechanical pressure, these are: no breathing (NB), negative gas adsorption (NGA), positive gas adsorption (PGA) and no op–to–cp transition (NB2). For these materials, these windows are always present, however, their boundaries depend on the host rigidity, adsorption strength, pore volume and guest interaction and size. In case of a type IIb material, we found a second region of negative gas adsorption (NGA2) in between the PGA and NB2 regions. The precise values of the pressures found here for the various materials might be sensitive to the force field and Van der Waals model used to parameterize the mean-field model. Furthermore, we also limited the investigation here to adsorption of guests above their critical temperature (by modifying the van der Waals *a* parameter). However, such technicalities do not undermine the conceptual introduction of various regimes that can clearly be identified in all these materials.

As a result, if one considers a material for which the pressure-induced breathing of the empty host is known (i.e., we know the type of the material) and the adsorption-induced breathing in the absence of an additional mechanical pressure is known (i.e., we know in which region the material is at $P_{\mathrm{mech}} = 0$), we can determine whether or not increasing the mechanical pressure could give rise to PGA/NGA or not. For example, the hypothetical system inspired by CH_4 in DUT-49 is a type IIa material that exhibited adsorption-induced breathing with negative gas adsorption in the absence of mechanical pressure, i.e., at $P_{\mathrm{mech}} = 0$ the system is in the NGA region. Hence, the model predicts that by applying an appropriately large mechanical pressure, the NGA behavior can be changed towards PGA. On the other hand, consider adsorption of CH_4 in MIL-53(Cr), i.e., a type III material that exhibits no breathing in absence of mechanical pressure. It was found that by means of applying an appropriately large mechanical pressure, breathing can be induced in this material featuring negative gas adsorption. Finally, consider adsorption of CO_2 in MIL-53(Cr), i.e., a type III material that exhibits PGA in absence of mechanical pressure. In this case, the model predicts that applying a positive mechanical pressure will not be able to induce NGA. Furthermore, we can now also understand why the DUT–48 framework synthesized by Krause et al.[27] does not exhibit any breathing transitions. Due to the shorter linker of the DUT–48 framework, it was found to be more rigid than DUT–49 (which is type IIa). As a result, the breathing regions of DUT-48 will be shifted towards higher pressures compared to DUT–49, as was illustrated in Fig. 5. Furthermore, the adsorption energy was also found to be smaller in DUT-48, which also compresses and further shifts the breathing region towards higher pressures. If these shifts are large enough (i.e., the stiffening of DUT–48 and/or decrease in adsorption energy is large enough compared to DUT–49), the NGA region may have shifted from including $P_{\mathrm{mech}} = 0$ (i.e., NGA observed in absence of mechanical pressure) to entirely to the right of $P_{\mathrm{mech}} = 0$ (i.e., no breathing transitions observed in absence of mechanical pressure). This also implies that if an appropriate (positive) external pressure is applied to DUT–48, it should again exhibit NGA, but this has not yet been validated experimentally to the best of our knowledge.

In conclusion, even though NGA was experimentally observed for methane adsorption in DUT-49, we herein discovered that it could be a more generally applicable phenomenon under influence of guest adsorption and external mechanical pressure. The application of the thermodynamic model for adsorption in soft porous crystals of type II or III revealed the existence of regions of distinct adsorption-induced breathing behavior as function of an applied mechanical pressure. These regions correspond to no breathing (NB and NB2), breathing with negative gas adsorption (NGA and NGA2) and breathing with positive gas adsorption (PGA). Although the specific mechanical pressure range of each region might change for different systems, the sequence of these regions is determined by its type, i.e., pressure-induced breathing behavior. Therefore, the ability for a system to undergo negative gas adsorption in absence of an external mechanical pressure is indeed dependent on the specific system. However, NGA might become tunable. For example, for systems that do not exhibit breathing in the absence of mechanical pressure, NGA should also be observed when an appropriate mechanical pressure is applied. Even though it is very difficult to indeed perform the required experiments to test such statements with the currently available experimental setups, it still allows us to gain crucial insight into the NGA phenomenon. More specifically, if one considers that the application of positive mechanical pressure can be regarded as making the material more flexible, one can clearly identify the degree of flexibility as one of the key features in exhibiting NGA. By performing the thought experiment of applying mechanical pressure, one can then easily identify whether a specific material is either to stiff or to flexible to observe NGA. Moreover, the sensitivity analysis also illustrated that the extent of the NGA region can be tuned by varying for example the adsorption interaction strength. Such observations help to identify the modifications to the material that are required to be able to exhibit NGA even in the absence of mechanical pressure. This in term could then open the way for various high-end applications such as tunable gas detection and pressure amplification.

Methods

Thermodynamic model. To compute adsorption isotherms and investigate the underlying reasons for negative gas adsorption, the mean field model derived by the present authors for single–component adsorption of guests in MOFs[31,37] will be applied. All derivations within this model are given in Supplementary Note 2, here we summarize the most important results. The model starts by expanding the Helmholtz free energy F of the system in terms of the empty host free energy (F_{host}), the free energy of a van der Waals gas confined within the pores (F_{guest}) and the free energy of interaction between the host and guests (F_{ads}):

$$\begin{aligned} F(N,V) &= F_{\text{host}}(V) + F_{\text{guest}}(N,V) + F_{\text{ads}}(N,V) \\ F_{\text{guest}}(N,V) &= k_{\text{B}}T\ln N! - Nk_{\text{B}}T\ln\left(\tfrac{V_{\text{p}}(V)-bN}{b}\right) \end{aligned} \quad (2)$$

$$-\frac{aN^2}{V_{\text{p}}(V)} + N\mu_0 \quad (3)$$

$$F_{\text{ads}}(N,V) = N\cdot\Delta U_{\text{ads}}(V) \quad (4)$$

where N represents the number of guest molecules adsorbed in the MOF, V is the unit cell volume, $V_{\text{p}}(V)$ represents the pore volume in which the adsorbed molecules are allowed to move, $\Delta U_{\text{ads}}(V)$ is the average adsorption energy of a single guest molecule and $\mu_0 = k_{\text{B}}T\ln\left(\frac{\Lambda^3}{b}\right)$ is a reference chemical potential corresponding to an ideal gas at a gas density of one particle per volume b and pressure of $\frac{k_{\text{B}}T}{b}$. Without any loss of generality, the number of unit cells was set to one and the temperature T is considered fixed (and no longer taken up as variable in the notation). Finally, the pore volume $V_{\text{p}}(V)$ will be described by a stepwise linear function, which is indeed a sufficient approximation (as is illustrated in Supplementary Note 4):

$$V_{\text{p}}(V) = s(V - V_0) \quad (5)$$

with $s = 0$ for $V < V_0$ and s a positive non-zero value for $V \geq V_0$. After expressing chemical equibrium with a given chemical potential μ several grand canonical quantities can be derived. First, the number of adsorbed particles:

$$N(\mu,V) = f(\mu,V)\cdot\frac{V_{\text{p}}(V)}{b} \quad (6)$$

with the fill factor f as a solution of the following equation:

$$\ln\left(\frac{f}{1-f}\right) + \frac{f}{1-f} - cf = \frac{\mu - \mu_0 - \Delta U_{\text{ads}}(V)}{k_{\text{B}}T} \quad (7)$$

and $c = \frac{2a}{k_{\text{B}}Tb}$. Second, the pressure:

$$\begin{aligned} P(\mu,V) = P_{\text{host}}(V) &+ P_0\left[\tfrac{f(\mu,V)}{1-f(\mu,V)} - \tfrac{c}{2}f^2(\mu,V)\right] \\ &- P_0 f(\mu,V)u(V) \end{aligned} \quad (8)$$

with $P_0 = s\frac{k_{\text{B}}T}{b}$ and $u(V) = \frac{V-V_0}{k_{\text{B}}T}\frac{\partial\Delta U_{\text{ads}}}{\partial V}$. Third, the grand canonical potential:

$$\Omega(\mu,V) = F_{\text{host}}(V) - P_0(V-V_0)\left[\frac{f(\mu,V)}{1-f(\mu,V)} - \frac{c}{2}f^2(\mu,V)\right] \quad (9)$$

Finally, after also applying mechanical equilibrium with a given pressure P, the following osmotic quantities can be derived. First, the unit cell volume $V(\mu, P)$ can be derived by solving following equation:

$$P = P_{\text{host}}(V) + P_0\left[\frac{f(\mu,V)}{1-f(\mu,V)} - \frac{c}{2}f^2(\mu,V)\right] - P_0 f(\mu,V)u(V) \quad (10)$$

Second, the number of adsorbed particles:

$$N(\mu,P) = f(\mu,V(\mu,P))\cdot\frac{V_{\text{p}}(V(\mu,P))}{b} \quad (11)$$

Third, the osmotic potential:

$$\begin{aligned} X(\mu,P) = F_{\text{host}}(V(\mu,P)) &+ PV(\mu,P) \\ &- P_0(V-V_0)\left[\tfrac{f(\mu,V(\mu,P))}{1-f(\mu,V(\mu,P))} - \tfrac{c}{2}f^2(\mu,V(\mu,P))\right] \end{aligned} \quad (12)$$

Computational details. The thermodynamic model requires input profiles for the empty host material ($F_{\text{host}}(V)$), pore volume ($V_{\text{p}}(V)$) and interaction energy ($\Delta U(V)$) as well as van der Waals a and b parameters. For DUT–49, $F_{\text{host}}(V)$ was constructed with a newly developed force field using QuickFF[38,39] (more details can be found in Supplementary Note 3), $\Delta U(V)$ was computed by means of the Monte Carlo scheme outlined in ref. [37] using the Universal Force Field[40] for the van der Waals interactions and atomic charges derived using the Minimal Basis Iterative Stockholder (MBIS) method[41] to model the electrostatic interactions, and the pore volume was fitted to the experimental measurements from ref. [22] For MIL-53(Cr) all input was taken from ref. [37]. For MIL-53(Al) the free energy of the empty host was constructed using a QuickFF force field taken from ref. [39], while the profiles for the adsorption energy and pore volume were computed using the scheme of ref. [37] with the same force field that was applied for the computation of the free energy profile (augmented with the MM3 parameters and MBIS gaussian charges for methane and carbon dioxide). The van der Waals parameters of the equation of state for methane and carbon dioxide were taken to be the same as used in refs. [31,37]. As mentioned before, the model can only be applied for temperatures above the critical temperature. Therefore, to simulate CH_4 at 120 K, its van der Waals a parameter was reduced so that the critical temperature reduces from 192 K to 80 K. Similarly, to simulate CO_2 at 300 K its van der Waals a parameter was very slightly reduced so that the cricital temperature reduces from 306 K to 299 K. Finally, the solution of the thermodynamic equations for the construction of grand canonical profiles, osmotic adsorption isotherms and breathing regions was done using an in-house developed python package.

Data Availability

The input data required for the thermodynamic model as well as the output datasets generated during and/or analysed during the current study using the thermodynamic model are available from the corresponding author upon request. See Supplementary Note 7 for more details.

Code Availability

The thermodynamic model applied in this work is implemented in a custom-written Python package which is available from the corresponding author upon request. See Supplementary Note 7 for more details.

Received: 12 November 2018 Accepted: 16 July 2019
Published online: 02 September 2019

References

1. Morris, R. & Brammer, L. Coordination change, lability and hemilability in metal-organic frameworks. *Chem. Soc. Rev.* **46**, 5444–5462 (2017).

2. Rogge, S. M. J. et al. Metal-organic and covalent organic frameworks as single-site catalysts. *Chem. Soc. Rev.* **46**, 3134–3184 (2017).
3. Howarth, A. J. et al. Chemical, thermal and mechanical stabilities of metal-organic frameworks. *Nat. Rev. Mater.* **1**, 15018 (2015).
4. Bennett, T. D., Cheetham, A. K., Fuchs, A. H. & Coudert, F.-X. Interplay between defects, disorder and flexibility in metal-organic frameworks. *Nat. Chem.* **9**, 11–16 (2016).
5. Yot, P. G. et al. Mechanical energy storage performance of an aluminum fumarate metal-organic framework. *Chem. Sci.* **7**, 446–450 (2016).
6. Horcajada, P. et al. Metal-organic frameworks in biomedicine. *Chem. Rev.* **112**, 1232–1268 (2012).
7. Li, J.-R. et al. Selective gas adsorption and separation in metal-organic frameworks. *Chem. Soc. Rev.* **38**, 1477–1504 (2009).
8. Lennox, M. J. & Düren, T. Understanding the kinetic and thermodynamic origins of xylene separation in UiO-66(Zr) via molecular simulation. *J. Phys. Chem. C* **120**, 18651–18658 (2016).
9. Hobday, C. L. et al. Understanding the adsorption process in ZIF-8 using high pressure crystallography and computational modelling. *Nat. Commun.* **9**, 1429 (2018).
10. Horike, S., Shimomura, S. & Kitagawa, S. Soft porous crystals. *Nat. Chem.* **1**, 695–704 (2009).
11. Schneemann, A. et al. Flexible metal-organic frameworks. *Chem. Soc. Rev.* **43**, 6062–6096 (2014).
12. Ghoufi, A., Benhamed, K., Boukli-Hacene, L. & Maurin, G. Electrically induced breathing of the mil-53(cr) metal-organic framework. *ACS Centr Sci.* **3**, 394–398 (2017).
13. Férey, G. Hybrid porous solids: past, present. *Future Chem. Soc. Rev.* **37**, 191–214 (2008).
14. Férey, G. et al. Why hybrid porous solids capture greenhouse gases? *Chem. Soc. Rev.* **40**, 550–562 (2011).
15. Coudert, F.-X. Metal-organic frameworks: the pressure is on. *Acta Crystallogr. B* **71**, 585–586 (2016).
16. Ogborn, J. M., Collings, I. E., Moggach, S. A., Thompson, A. L. & Goodwin, A. L. Supramolecular mechanics in a metal-organic framework. *Chem. Sci.* **3**, 3011–3017 (2012).
17. Li, W. et al. Negative linear compressibility of a metal-organic framework. *J. Am. Chem. Soc.* **134**, 11940–11943 (2012).
18. Wu, Y. et al. Negative thermal expansion in the metal-organic framework material cu3(1,3,5-benzenetricarboxylate)2. *Angew. Chem. Int. Ed.* **47**, 8929–8932 (2008).
19. Zhou, W., Wu, H., Yildirim, T., Simpson, J. R. & Walker, A. R. H. Origin of the exceptional negative thermal expansion in metal-organic framework-5 Zn_4O(1,4-benzenedicarbolxylate)$_3$. *Phys. Rev. B* **78**, 054114 (2008).
20. Goodwin, A. L. & Kepert, C. J. Negative thermal expansion and low-frequency modes in cyanide-bridged framework materials. *Phys. Rev. B* **71**, 140301 (2005).
21. Cliffe, M. J., Hill, J. A., Murray, C. A., Coudert, F.-X. & Goodwin, A. L. Defect-dependent colossal negative thermal expansion in uio-66(hf) metal-organic framework. *Phys. Chem. Chem. Phys.* **17**, 11586–11592 (2015).
22. Krause, S. et al. A pressure-amplifying framework material with negative gas adsorption transitions. *Nature* **532**, 348–352 (2016).
23. Salles, F. et al. Multistep n2 breathing in the metalorganic framework co(1,4-benzenedipyrazolate). *J. Am. Chem. Soc.* **132**, 13782–13788 (2010).
24. Evans, J. D., Bocquet, L. & Coudert, F.-X. Origins of negative gas adsorption. *Chemistry* **1**, 873–886 (2016).
25. Evans, J. D., Krause, S., Kaskel, S., Sweatman, M. B. & Sarkisov, L. Exploring the thermodynamic criteria for responsive adsorption processes. *Chem. Sci.* **10**, 5011–5017 (2019).
26. Schaber, J. et al. In situ monitoring of unique switching transitions in the pressure amplifying flexible framework material DUT-49 by high-pressure Xe-129 NMR spectroscopy. *J. Phys. Chem. C* **121**, 5195–5200 (2017).
27. Krause, S. et al. Adsorption contraction mechanics: understanding breathing energetics in isoreticular metal-organic frameworks. *J. Phys. Chem. C* **122**, 19171–19179 (2018).
28. Krause, S. et al. The effect of crystallite size on pressure amplification in switchable porous solids. *Nat. Commun.* **9**, 1573 (2018).
29. Dechnik, J., Gascon, J., Doonan, C. J., Janiak, C. & Sumby, C. Mixed-matrix membranes. *Angew. Chem. Int. Ed.* **56**, 9292–9310 (2017).
30. Vanduyfhuys, L. et al. Thermodynamic insight into stimuli-responsive behavior of soft porous crystals. *Nat. Commun.* **9**, 204 (2018).
31. Vanduyfhuys, L., Ghysels, A., Rogge, S., Demuynck, R. & Van Speybroeck, V. Semi-analytical mean-field model for predicting breathing in Metal-Organic Frameworks. *Mol. Simula.* **41**, 1311–1328 (2015).
32. Huber, P. & Knorr, K. Adsorption-desorption isotherms and x-ray diffraction of ar condensed into a porous glass matrix. *Phys. Rev. B* **60**, 12657–12665 (1999).
33. Gor, G. Y. et al. Elastic response of mesoporous silicon to capillary pressures in the pores. *Appl. Phys. Lett.* **106**, 261901 (2015).
34. Gor, G. Y., Huber, P. & Bernstein, N. Adsorption-induced deformation of nanoporous materials-a review. *Appl. Phys. Rev.* **4**, 011303 (2017).
35. Evans, R., Marconi, U. M. B. & Tarazona, P. Capillary condensation and adsorption in cylindrical and slit-like pores. *J. Chem. Soc.* **82**, 1763–1787 (1986).
36. Ravikovitch, P. I. & Neimark, A. V. Density functional theory of adsorption in spherical cavities and pore size characterization of templated nanoporous silicas with cubic and three-dimensional hexagonal structures. *Langmuir* **18**, 1550–1560 (2002).
37. Ghysels, A. et al. On the thermodynamics of framework breathing: a free energy model for gas adsorption in MIL-53. *J. Phys. Chem. C.* **117**, 11540–11554 (2013).
38. Vanduyfhuys, L. et al. QuickFF: A program for a quick and easy derivation of force fields for Metal-Organic Frameworks from ab initio input. *J. Comput. Chem.* **36**, 1015–1027 (2015).
39. Vanduyfhuys, L. et al. Extension of the QuickFF force field protocol for an improved accuracy of structural, vibrational, mechanical and thermal properties of metal-organic frameworks. *J. Comput. Chem.* **39**, 999–1011 (2018).
40. Rappé, A. K., Casewit, C. J., Colwell, K. S., Goddard, W. A. & Skiff, W. M. UFF, a full periodic table force field for molecular mechanics and molecular dynamics simulations. *J. Am. Chem. Soc.* **114**, 10024–10035 (1992).
41. Verstraelen, T. et al. Minimal basis iterative stockholder: atoms in molecules for force-field development. *J. Chem. Theory Comput.* **12**, 3894–3912 (2016).

Acknowledgements

This work is supported by the Fund for Scientific Research Flanders (FWO) and the Research Board of Ghent University (BOF). V.V.S. acknowledges funding from the European Union's Horizon 2020 research and innovation programme (consolidator E.R.C. grant agreement No 647755 - DYNPOR (2015-2020)). The computational resources (Stevin Supercomputer Infrastructure) and services used in this work were provided by the VSC (Flemish Supercomputer Center), funded by Ghent University, FWO and the Flemish Government - department EWI. We wish to acknowledge Jelle Wieme for deriving the QuickFF force field for DUT-49.

Author contributions

L.V. and V.V.S. initiated the discussion, designed the paper, discussed the results and wrote the manuscript. L.V. implemented the thermodynamic model and performed the simulations.

Additional information

Supplementary information accompanies this paper at https://doi.org/10.1038/s42005-019-0204-y.

Competing interests: The authors declare no competing interests.

Reprints and permission information is available online at http://npg.nature.com/reprintsandpermissions/

Publisher's note: Springer Nature remains neutral with regard to jurisdictional claims in published maps and institutional affiliations.